



City Research Online

City, University of London Institutional Repository

Citation: Corlho, L., Placidi, M., Atkin, C.J. & Sun, Z. (2016). Experimental Investigation of a Handley Page Triple Slotted Aerofoil. Paper presented at the 2016 Applied Aerodynamics Conference: Evolution & Innovation Continues - The Next 150 Years of Concepts, Design and Operations, 19-21 July 2016, Bristol, UK.

This is the accepted version of the paper.

This version of the publication may differ from the final published version.

Permanent repository link: <https://openaccess.city.ac.uk/id/eprint/15673/>

Link to published version:

Copyright: City Research Online aims to make research outputs of City, University of London available to a wider audience. Copyright and Moral Rights remain with the author(s) and/or copyright holders. URLs from City Research Online may be freely distributed and linked to.

Reuse: Copies of full items can be used for personal research or study, educational, or not-for-profit purposes without prior permission or charge. Provided that the authors, title and full bibliographic details are credited, a hyperlink and/or URL is given for the original metadata page and the content is not changed in any way.

City Research Online:

<http://openaccess.city.ac.uk/>

publications@city.ac.uk

Experimental Investigation of a Handley Page Triple Slotted Aerofoil

Lazaro Coelho, Marco Placidi, Chris Atkin and Zhengzhong Sun
Department of Mechanical Engineering & Aeronautics, City University London, London, UK

Abstract

A triple slotted aerofoil following the Handley Page 44F design was tested at City University London T-2 wind tunnel. The model allowed the study of a fixed triple slotted wing as well as investigation of the effects of isolated slots at different locations along the chord. PIV measurements were performed within the chord Reynolds number range in between approximately 200,000-400,000. The model was tested at an angle of attack of 22° . Measurements of mean streamwise velocity, velocity fluctuations and shear stress were analysed. The study shows how an isolated slot is more favourable when it is placed closest to the leading edge, although slow moving fluid regions can still be found close to the trailing edge. Fully attached flow was only achievable by using all three slots. In addition, the fully slotted profile is shown to generate channel exit velocities in the order of $1.4U_\infty$, which highly energise the boundary layer on the suction side.

1 - Introduction

Flow control is employed to improve the aerodynamic performance of aircrafts' wings. It can be realised via the use of auxiliary aerofoils (Chen [1]), boundary layer injection/suction (Shojaerfard, *et al* [2]) or vortex generators (Johnston [3]). Studies on auxiliary aerofoils (Lachman [4], Handley Page [5], Wenzinger, C., *et al* [6]) culminated in the development of high-lift systems (HLSs), namely slats and flaps, which are currently used in most commercial passenger airliners. The deployment of these auxiliary aerofoils changes the overall wing geometry and the pressure distribution on the constituent elements resulting in increased lift coefficient, C_L (at a price of increased drag). In addition, the convergent shape of the channel formed between the slat/flap and the subsequent aerofoil makes use of the pressure differential to drive and accelerate the passing air, which is shown to be beneficial for the flow development as it contributes for attached flow and thus prevents separation (van Dam, C.P. [7]). A large amount of work with respect to the common HLS is present in the literature (Chen [1], van Dam, C.P. [7]). With regards to the deployable slat, not only its geometry and positioning of the latter in relation to the main aerofoil is of importance, but also when deployed, the events taking place in the cove region necessary to allow these HLSs to be retracted. These complex highly recirculating flow regions result in a high-noise signature and also present a challenge for flow simulation, which results in difficulties in multi-element aerofoil modelling (Olson, L., *et al* [8], Tung, C., *et al* [9], Savory, E. *et al* [10]). Moreover, complex mechanical actuators need to be designed and implemented to allow deployment. The fixed leading edge slat, however, has the benefit of requiring neither a cove region nor a mechanical actuator, while positively contributing to the flow development due to the above cited reasons. In addition, Katzmayer and Kirste [4] concluded that generally an auxiliary fixed HLS produces better results than a retractable slat because of the lack of the cove region.

Recently, the interest in a fixed leading edge slot has grown due to its potential application for wind turbines, as it has been demonstrated efficient in both preventing flow separation and increasing the overall aerodynamic efficiency (Ashworth [12], Weick [13]). Also, modern flow field analysis of this type of configurations are lacking in the literature as a means to further understand the behaviour of the flow over such aerofoils.

Therefore, the present investigation was intended to determine the effect of the fixed leading edge slot on the flow field and to observe the correlation between slot location and separation reduction over an aerofoil at a high angle of attack by means of digital flow field capture. Three different slot locations along the chord are investigated in this study. In addition, the flow field around a triple slotted wing is visualised to understand the impact of the slots.

2 – Experimental facility and details

The slotted aerofoil under investigation follows the design of Handley Page. This was achievable, thanks to the kind support of the HP foundation, which agreed on make the original model available to City University. A sketch of the model can be seen in figure 1.

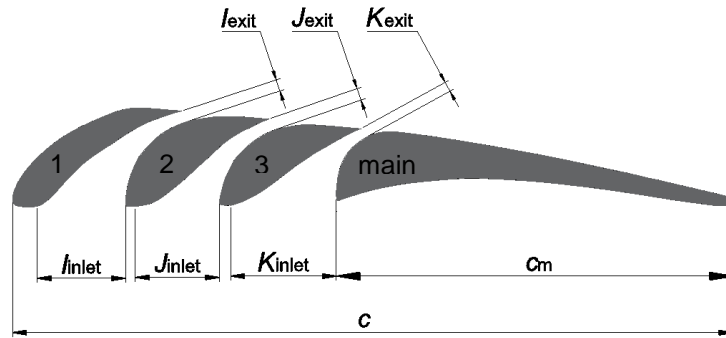


Figure 1. Geometry of the HP 44F triple slotted aerofoil.

The model comprises one major section and three smaller front aerofoils ('main' and 1, 2 and 3 respectively in figure 1). Hence, three leading edge slots I, J, K are formed throughout the whole span of 500mm. The chord of the aerofoil is $c=153.8$ mm in length; where the chord c_m of the main aerofoil is 84.6mm ($0.55 x/c$) and the geometric characteristics of the slots can be found in table 1.

Slot	Inlet (x/c)	Exit (x/c)	Inlet/Exit Ratio	Exit location (x/c)
I	0.123	0.016	7.7:1	0.24
J	0.117	0.017	6.9:1	0.36
K	0.147	0.013	11.3:1	0.5

Table 1 – Geometric characteristics of the experimental model.

The channel inlet dimensions are taken from the points where the slotted aerofoil deviates from the solid contour and the exit dimensions are aligned with the exit orientation (as shown in figure 1).

The experiments were performed in the T-2 wind tunnel at City University London. The test section of the latter measures 1.12 m x 0.81 m x 1.78 m and the freestream turbulence intensity is $<0.8\%$, which is deemed appropriate for the current experiment. The tunnel was operated at 20 m/s, 30m/s and 40 m/s resulting in a Reynolds number Re_c in the range of 200,000-400,000.

In this study, we use x, y, z to indicate the streamwise, wall-normal and spanwise directions. Mean velocity along this axis is indicated by U, V, W , while fluctuating components are denoted as U', V', W' . In order to generate substantial flow recirculation over the suction side of the aerofoil, the model is installed at an angle of attack (AoA) of 22 degrees. Particle Image Velocimetry (PIV) is employed to capture velocity fields. The experimental setup with the aerofoil model, laser sheet and camera are shown in figure 2.

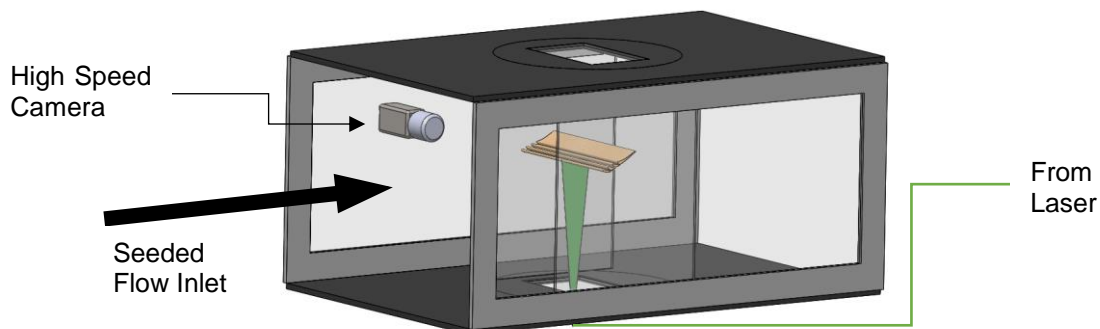


Figure 2. Schematic of experimental setup. AoA 22°.

The aerofoil was mounted horizontally in the centre of the test section and supported by Perspex plates to suppress any 3D flow effects. To prevent deflection of the constituent aerofoils under load, small plastic clips were used to support them in the centre. The present aerofoil allows the study on the slots location effect through opening/closing individual sections. The examined cases are shown in figure 3.

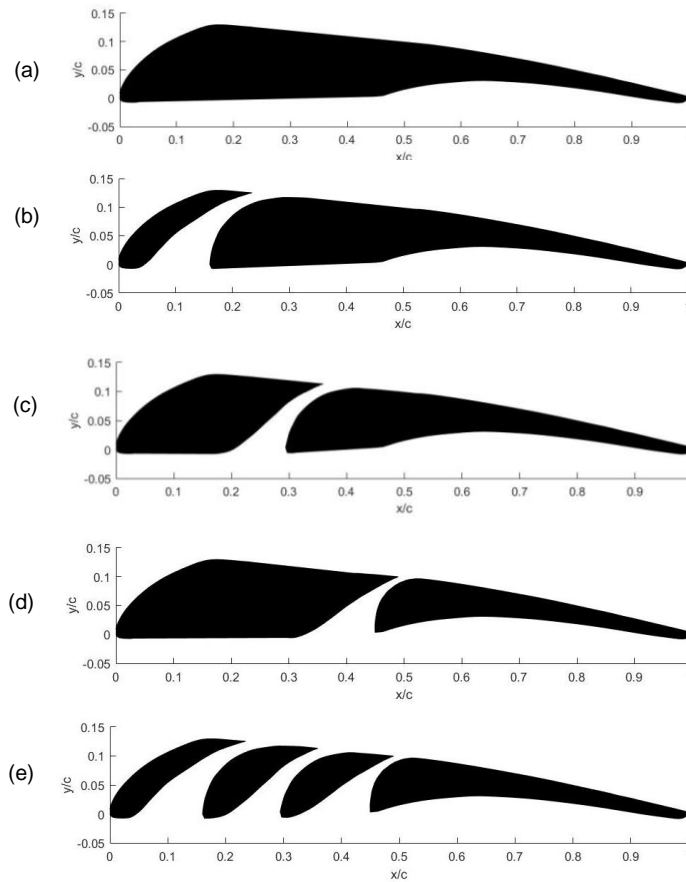


Figure 3. Studied configurations (a) solid (b) slot 1 open (c) slot 2 open (d) slot 3 open (e) triple or fully slotted.

A Phantom M310 CMOS high-speed camera with a resolution of 1280×800 pixels², equipped with a Nikon 100 mm lens was used for particle imaging. A Litron LDY300 series dual-pulsed laser was used to illuminate the particles. A periscopic laser beam delivery arm with a combination of optics was used to form the laser sheet and to direct it into the wind tunnel test section through the bottom wall, which offers optical access. A Laskin 9307-6 oil droplet generator was used to generate seeding particles (olive oil), which have a nominal diameter of approximately $1 \mu\text{m}$. A high-speed synchroniser (TSI 610036) was used to trigger the camera and the laser.

A 1000 frame set was acquired for each configuration to promote converging statistics. Each image pair was captured with a time interval between $5 \mu\text{s}$ and $15 \mu\text{s}$ depending on the flow velocity.

Given the limitations in optics and camera availability, it was necessary to join two or more field of views (FOVs) to obtain the entire flow field around the region of interest. In addition, the camera had to be moved for each configuration, which resulted in slightly different resolved FOV for each case. These factors resulted in different unresolved regions, as it becomes apparent in subsequent figures. The FOVs used for the different configurations can be seen in figure 4.

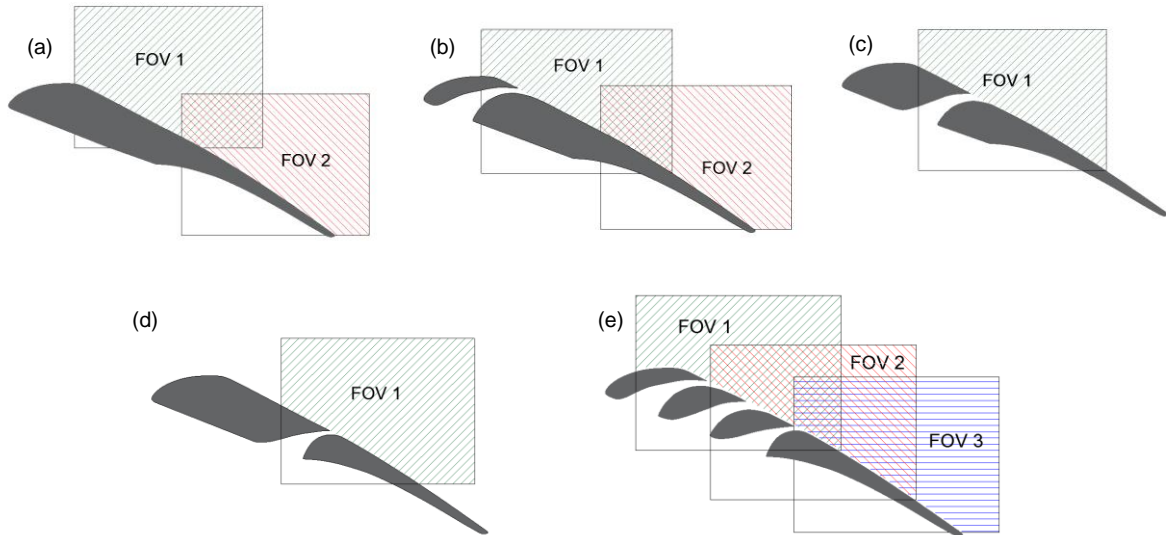


Figure 4. Field of view (FOVs) for (a) solid (b) slot 1 open (c) slot 2 open (d) slot 3 open (e) slotted cases.

TSI InSight 4G software was used to capture the images and generate the vector fields. Image pre-processing entailed the subtraction of minimum intensity background noise. Spurious vectors generated by laser light reflection, low seeding density, etc. were removed and replaced by statistical generated vectors.

3 - Results and discussion

Section 3.1 discusses contours of mean velocity fields, which allowed comparison of the behaviour of the flow in the presence and absence of the slots. Section 3.2 considers the mean velocity fluctuations, while section 3.3 contains contours of the shear stress. Instantaneous velocity fields are analysed in section 3.4, which aids to visualise the flow patterns emerging from the slots.

3.1 - Mean velocity fields

Figure 5 shows the flow features of the solid aerofoil (slots closed), here taken as benchmark case. At the chosen angle of attack (22 degrees) this case is not able to sustain attached flow over the suction side and significant flow separation is observed. The same behaviour was observed at all tested velocities. The overlaid velocity vector field (in white) aids visualising the recirculation bubble. This is centred close to the aerofoil trailing edge and has height of $0.3c$ with reversed flow up to a magnitude of $0.2 U_\infty$. Moreover, the onset of separation is rather early, in correspondence of what would be the location of the first slot (see figure 6(a) for comparison).

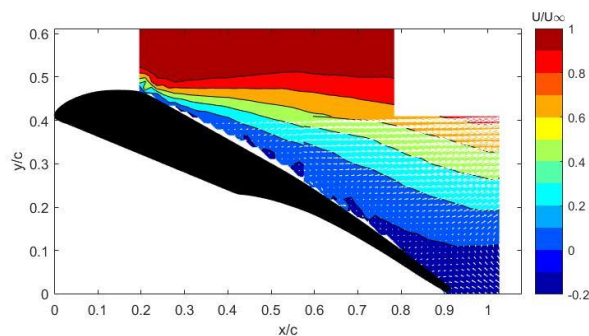


Figure 5. Contour of time-averaged streamwise velocity component U/U_∞ at $AoA=22^\circ$ for solid aerofoil; $U_\infty=40$ m/s
Velocity vectors are visualized by white arrows.

Figure 6 shows mean velocity contours for the remaining test cases.

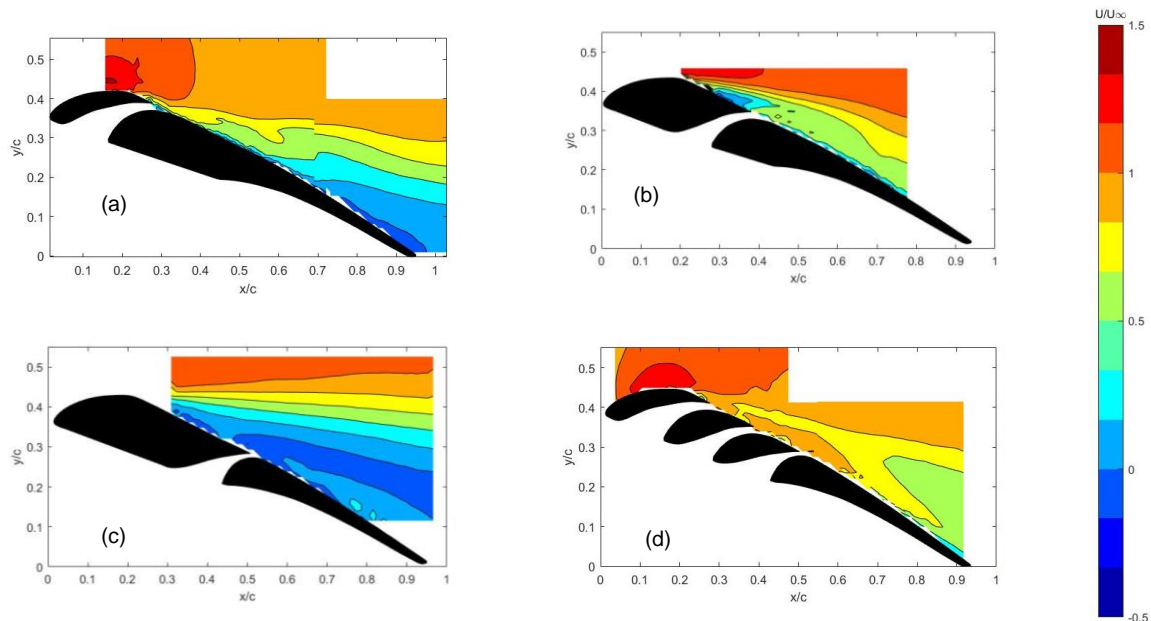


Figure 6. Contour of time-averaged streamwise velocity component U/U_∞ at $AoA=22^\circ$ for (a) slot 1 open (b) slot 2 open (c) slot 3 open (d) slotted; $U_\infty=40$ m/s.

Opening of the first leading edge slot is expected to alleviate flow separation, as a high-momentum jet should entrain the external flow. It is shown in figure 6(a) that this high-momentum flow re-energises the boundary layer, resulting in reducing the large-scale separation, when compared to previous case in figure 5. It is apparent that the boundary layer re-develops after the first slot and remains attached for the most part of the upper surface, despite the existence of a small packet containing reversed flow at the trailing edge. However, the re-developed boundary layer is not able to fully overcome the large turning angle and only has velocity magnitude of $0.2U_\infty$ at the trailing edge. This could lead to unsteadiness and flow separation if adverse pressure gradient is further encountered or the AoA is slightly increased. Further, when tested at 20 m/s, this configuration revealed separated flow at the trailing edge, however this result is here omitted.

Figure 6(b) shows the effect of opening the second slot, which causes the development of attached flow over the trailing element with small high-velocity packets exiting the slot. A small separation bubble of height $0.05c$ can be seen in the upper surface prior to the slot exit before re-attachment is achieved. Although the slot contributes to keeping the flow attached in the region near the slot exit, the instantaneous flow field suggests further separation at the trailing edge under this configuration (although not shown here for the sake of brevity).

The effect of opening the third slot is shown in figure 6(c). It is clear that this position is not able to contribute to an attached flow. The flow remains separated although the velocity of the flow adjacent to the trailing element is seen to increase to $0.2U_\infty$. This could denote instabilities caused by the interaction of the recirculating flow and the flow exiting the channel.

Utilisation of the remaining two slots, namely slots 1 and 2 in figure 1, further improves the flow quality, as more high-momentum flow is entrained. The resulted flow field in the triple slotted configuration is shown in figure 6(d). The downstream flow velocity increases further to $0.7U_\infty$ close to the trailing edge. Moreover, high velocity is injected within the boundary layer and persists over a larger portion of the aerofoil. The slot jet has much more impact on the flow field, and the energised region is more apparent than that in flow when only one slot was open (figure 6(a)). To summarise, multiple slots are beneficial in consolidating the control outcome and the sole use of one slot (irrespective of its location) is shown not to fully succeed in keeping the flow attached. However, it is clear that the further upstream a single slot is located, the more beneficial its effect is. This is in accordance with the result from Weick and Shortall [13] on the Clark Y wing.

3.2 - Mean fluctuating fields

Figure 7 shows mean fluctuations of streamwise velocity for the solid case. These have peak values over $0.4U_\infty$ for $Re_c=4 \times 10^5$. This is in accordance with unsteadiness within the large separation region observed in the mean velocity contours in figure 5.

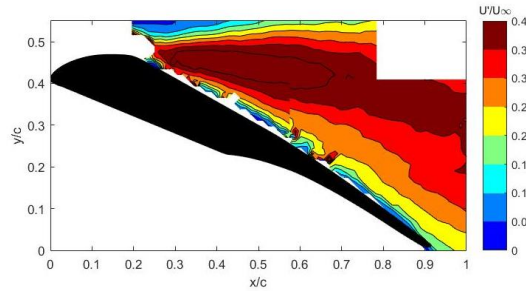


Figure 7. Contour of time-averaged streamwise normalised velocity fluctuation U'/U_∞ at $AoA=22^\circ$ for solid aerofoil.

Similar analysis is carried out for the slotted cases and it is presented in figure 8. Under the same conditions, the cases where the second and third slots are open (Figure 8(b)(c)) also experience high velocity fluctuations (of the order of $0.25U_\infty$) although these clearly diminish after the slot exit. Nevertheless, these two cases are characterised by separated flow close to the trailing edge. The velocity fields suggest that the further upstream the slot is located, the smaller the unstable flow region becomes. Opening of the first slot (in Figure 8(a)) removes instabilities at the leading edge and achieves attached flow. The fluctuations closer to the trailing edge move further away from the surface and when the model is fully slotted (Figure 8(d)) these instabilities become yet less severe. The maximum mean fluctuating magnitude sits close to $0.2U_\infty$ for the slotted case (Figure 8(d)) compared to a maximum of $0.25U_\infty$ for the case where the first slot is open (figure 8(a)). This suggests attached flow throughout the upper surface for the fully slotted configuration.

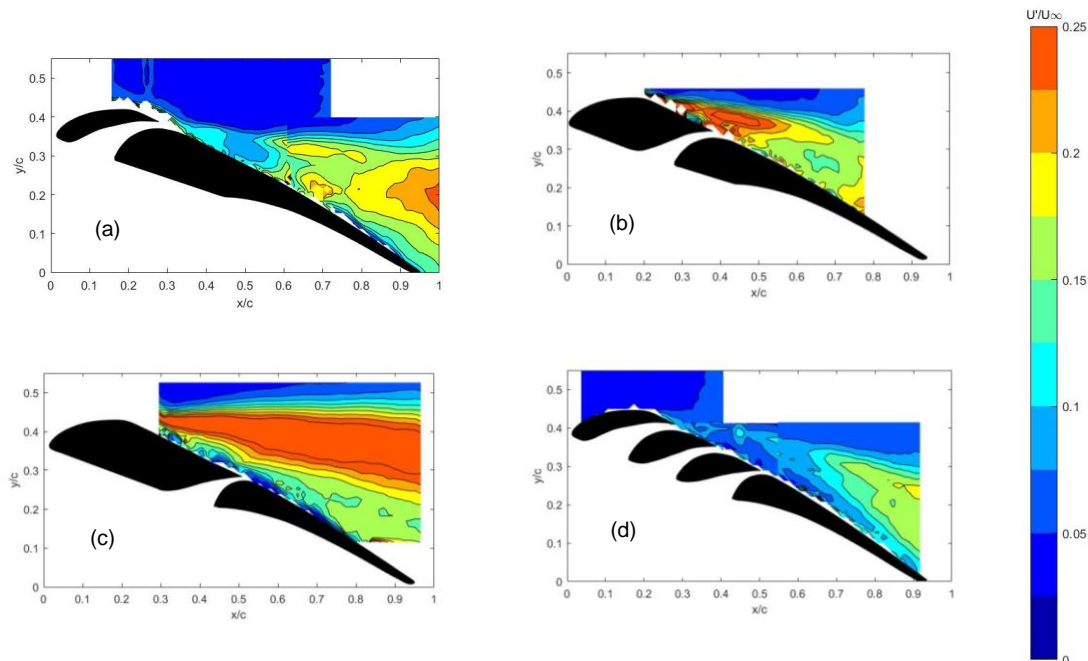


Figure 8. Contour of time-averaged streamwise normalised velocity fluctuation U'/U_∞ at $AoA=22^\circ$ for (a) slot 1 open (b) slot 2 open (c) slot 3 open (d) slotted; $U_\infty=40$ m/s.

3.3 - Shear stress fields

At each slot exit, a shear layer develops in between the channel flow and its surroundings due to the velocity differences. To examine the extent of the latter, shear flow fields are presented. The shear layer between the flow originating from the jets and the freestream can be seen becoming thinner as the location of the slot is moved towards the leading edge. The shear layer developed with slot 3 open, seen in figure 9(a) is that of a separated flow and reaches magnitude of $3 \times 10^{-3} U'V'/U_\infty^2$. With slot 2 open, a considerable reduction of the shear layer extent and magnitude is visible in figure 9(b). In addition, small packets of positive shear are seen close to the slot exit, which indicate the interference of the external flow with the flow exiting the slot.

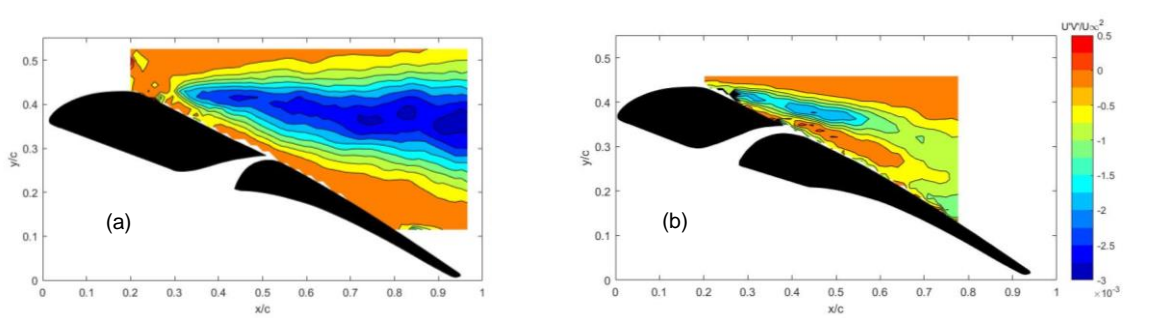


Figure 9. Contour of time-averaged normalized shear stress $U'V'/U_\infty^2$ at $AoA=22^\circ$ for (a) slot 3 open (b) slot 2 open; $U_\infty=40$ m/s.

Figure 10 shows the shear stress distribution for the cases where the first slot is open and for the fully slotted case in (a) and (b) respectively. These are plotted separately from the remaining cases due to the large difference in shear stress magnitudes observed.

A decrease of 50% in the maximum shear stress is observed upon opening of the first slot, as shown in figure 10(a). In addition, the shear layer seems to develop close to the trailing edge, in contrast with the cases where the slots were located further downstream, that originated a large shear region close to the leading edge. Employment of all three slots further decreases the shear stresses and only a thin shear layer, far from the aerofoil surface, is visible (Figure 10(b)). Moreover, the maximum shear stress is reduced by 30% when compared to the case where the first slot is open in (a). These findings show the favourable impact of implementing a fully slotted configuration where there is a much higher momentum transfer to the top surface keeping the flow attached.

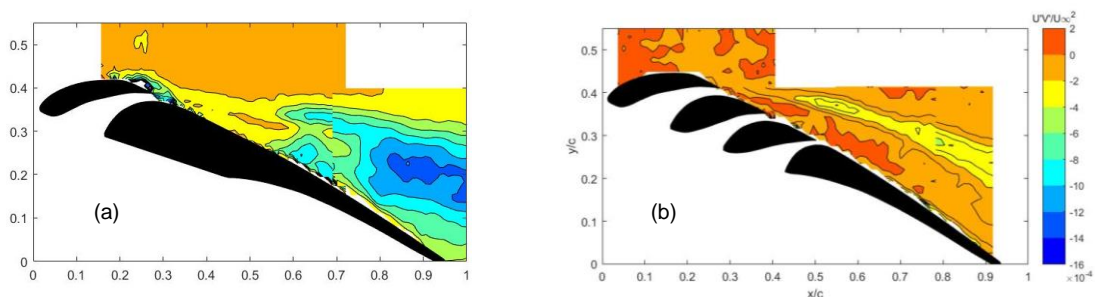


Figure 10. Contour of time-averaged normalized shear stress $U'V'/U_\infty^2$ at $AoA=22^\circ$ for (a) slot 1 open (b) slotted; $U_\infty=40$ m/s.

3.4 - Instantaneous flow fields

It has been shown so far that the jets exiting the channels are responsible for reattaching the flow at the trailing edge of the airfoil. To further explore this matter, instantaneous velocity fields are investigated, in the hope of offering further support to this hypothesis. The case where the second slot is open is depicted in figure 11, showing three consecutive snapshots (a), (b) and (c) to aid visualisation of the flow evolution along the chord. In this case, a separated flow region can be seen

on the upper surface just before the channel exit, being accelerated to $0.7U_\infty$ aft the channel exit. This causes the development of a new boundary layer at the trailing element and also the softening of the shear layer upstream. Further analysis of instantaneous velocity in this configuration shows the development of high fluctuations and vortical structures close to the trailing edge, which suggest further separation at that region, despite the beneficial effects of the slot.

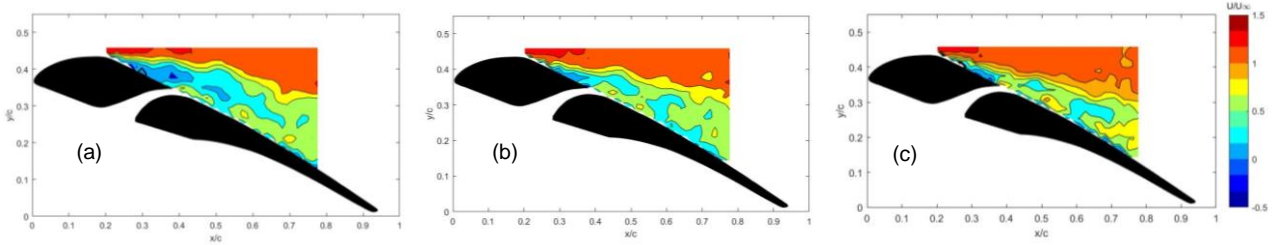


Figure 11. Contour of streamwise instantaneous velocity component U/U_∞ at $AoA=22^\circ$ for slot 2 open $U_\infty=40$ m/s.

Similarly, the three consecutive snapshots shown in figure 12 show the evolution of the flow field when the first slot is open. Slow moving fluid is seen close to the trailing edge and a large unstable region is found there, in accordance to findings shown in section 3.2. Small packets of fluid at velocity U_∞ are seen exiting the channel and contributing to reduce the low-momentum region downstream.

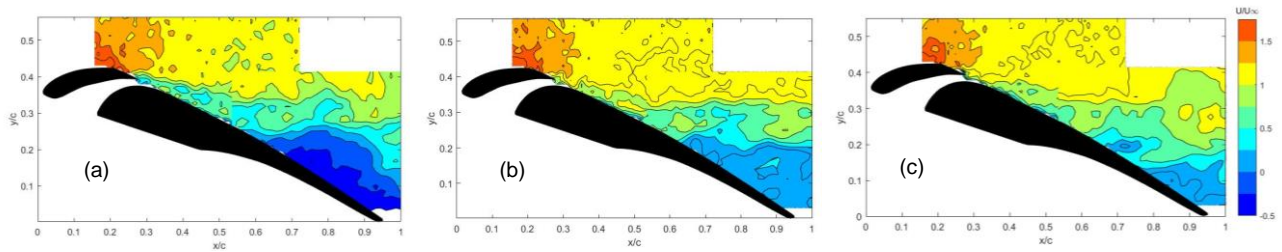


Figure 12 – Contour of streamwise instantaneous velocity component U/U_∞ at $AoA=22^\circ$ for slot 1 open aerofoil $U_\infty=40$ m/s.

Instantaneous velocity contours for the triple slotted case are shown in figure 13. These suggest a steady behaviour of the flow on the upper surface. The slots channels are seen to output flow at a velocity up to $1.4U_\infty$, which energises the fluid in the suction side. Flow deceleration is seen close to the trailing edge, although the boundary layer is still attached. This is in accordance to the shear layer developed in this configuration (as shown in figure 10(b)). This configuration exhibits the same behaviour at all the tested Reynolds numbers, which speaks for the consistency of the results.

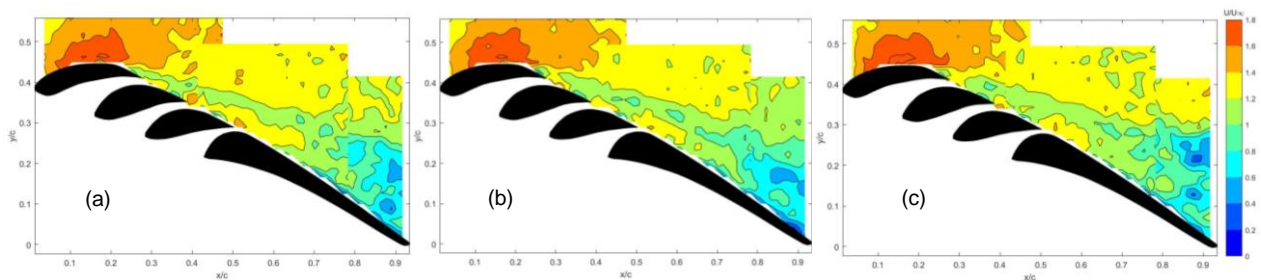


Figure 13 – Contour of streamwise instantaneous velocity component U/U_∞ at $AoA=22^\circ$ for slotted aerofoil $U_\infty=40$ m/s.

The slot exit velocity is seen to be higher for the slotted case when compared to the exit velocity when only one slot is opened. Hence, utilisation of all slots is shown to be the most favourable configuration to fully suppress flow separation. An interesting point is that the exit velocity at the first slot differs when subsequent slots are used. Also, we must recall the work of Lungstrom [11], who states that the gap between the slat and the main aerofoil must not be smaller than 2% chord to obtain favourable

results, and the work of Abbot and Von Doenhoff [14], who suggest that the optimum slot opening is in the order of 1% chord or slightly higher for flaps. In this experiment, the exit dimensions of 1.6%, 1.7% and 1.3% chord are shown to successfully energise the boundary layer despite that any variation to these parameters could not be investigated. In addition, for an isolated slot case, the channel exit velocity is seen to progressively decrease, as the channel is placed downstream. Again, this entails that the slot becomes more favourable as it is placed closer to the leading edge, in accordance with the work of Weick [13] on the slotted Clark Y wing. It is also shown in this work, however, that slots located further downstream are favourable, especially those located in the region 0.75-0.8c.

4 – Conclusions and further work

Wind tunnel experiments were performed to study control separation on a triple slotted aerofoil. These revealed the positive outcome of leading edge slots in doing so through PIV measurements.

In the present work, jet velocity at the slot outlet reaches values up to $1.4U_\infty$ and is capable of locally re-energising the boundary layer in the fully slotted configuration. When only one of the slots is used, the channel exit velocity is seen to reduce as the channel is progressively placed downstream, although a relationship between the slot position and effect on exit velocity showed no clear trends. For the case of the first slot open, the exit velocity was seen to be of the order of U_∞ and for the case of slot 2 open, the exit velocity was measured to be $0.7U_\infty$. This discrepancy is seen to have impact on the overall flow field given that, as a result, the region of separated flow is seen to grow. Flow separation can be prevented using solely the first slot, however, relatively low speed is still present in the flow field, which suggests that the flow is bound to separate due to unsteadiness. Nevertheless, this study concludes that upon using only one slot, the most beneficial location is that closest to the leading edge. Improved control, achieved by using all three slots, results in total separation suppression. Only this configuration withstands the pressure gradients characterising the model guaranteeing a fully attached flow.

Despite the exit velocity for the slotted case being the same for all channels (i.e. $1.4U_\infty$), additional studies considering opening of slots *I* and *J*, as well as *I* and *K* could shed more light into the influence of consecutive slots and the chord-wise distance between them. Further study on the aerodynamic performance of the cases presented herein via the use of a 6-component force balance is also scheduled in order to link the flow physics to the aerodynamic loads.

Acknowledgements

The authors are grateful to the support from the NWTF (under the EPSRC Grant Ref. EP/L024888/1) for some of the tunnel instrumentations and the Handley Page Foundation for making the HP 44F model available to City University London.

References

- 1 - Chen, A., "The determination of the geometries of multiple-element airfoils optimised for maximum lift coefficient", PhD Thesis, Dept. of Aeronautical and Astronautical Engineering, University of Illinois, 1971
- 2 – Shojaerfard, M., Noorpoor, A., Avanesians, A. Ghaffarpour, M., "Numerical investigation of flow control by suction and injection on a subsonic airfoil" *American journal of applied sciences* 2 Vol 10 pp1474-1480, 2005
- 3 – Johnston, J. Nishi, M., "Vortex generator jets – Means for flow separation control" *AIAA Journal*, Vol 28, No 6, pp. 989-994, 1990
- 4 – Lachmann, G., "Experiments with Slotted wings", *NACA Technical Note 71*, 1921
- 5 – Page, H., "Tests on an airfoil with two slots suitable for an aircraft of high performance", *NACA technical memorandum 369*, 1926

- 6 - Wenzinger, C., Shortal, J., "The aerodynamic characteristics of a slotted Clark Y wing as affected by the auxiliary airfoil position" *NACA report 400*, 1931
- 7 - van Dam, C. P. "The aerodynamic design of multi element high lift systems for transport airplanes" *Progress in Aerospace Sciences Vol 38* pp 101-144, 2002
- 8 - Olson, L., McGowan, P., Guest, C., "Leading edge slat optimization for maximum airfoil lift", *Nasa Technical Memorandum 78566*, 1979
- 9 – Tung, C., McAlister, K., Wang, G., "Unsteady aerodynamic behaviour of an aerofoil with and without a slat" *Computers Fluids Vol 22*, No 4/5, pp. 529-547, 1993
- 10 – Savory, E., Toy, N., Tahouri, B. Dalley, S., "Flow regimes in the cove regions between a slat and wing and between a wing and flap of a multi-element airfoil" *Experimental Thermal and Fluid Science Vol 5* pp. 307-316, 1992
- 11 - Lungstrom, B., "2D wind tunnel experiments with double and triple slotted flaps", Aeronautical research institute of Sweden, FFA-TN AU-993, 1973
- 12 – Ashworth, J., Whitman, N., Sparks, R., Ali, S. "Experimental Investigation of Slotted Airfoil Performance with Modified Slot Configurations" *24th AIAA Applied Aerodynamics Conference* June 2006.
- 13 – Weick, F., Shortal, J. "The effect of multiple fixed slots and a trailing edge flap on the lift and drag of a clark Y airfoil" *NACA Report 427*, 1933
- 14 – Abbot, I., Von Doenhoff, A., "*Theory of wing sections*" Dover Publications, New York, 1949